

ScienceDirect



IFAC PapersOnLine 55-13 (2022) 282-287

Unifying Energy-management Problems for Inverter-based Power Networks *

Manish K. Singh * D. Venkatramanan * Sairaj Dhople * Benjamin Kroposki ** Georgios B. Giannakis *

* University of Minnesota (UMN), Minneapolis, MN USA
(e-mails: msingh,dvenkat,sdhople,georgios@umn.edu)

** National Renewable Energy Laboratory (NREL), Golden, CO USA
(e-mail: benjamin.kroposki@nrel.gov)

Abstract: This paper outlines a suite of energy-management problems for inverter-based power networks from the vantage point of optimal control and (non)linear optimization. The problems are categorized based on timescales dictated by the network dynamics, and organized methodologically based on the problem complexity. A growing body of literature has addressed problems in this domain, albeit, with poorly motivated assumptions and behavioral models that obscure precise device behavior. With a combination of circuit- and control-theoretic lenses, we establish appropriate dynamic models for the networked resources, illustrate how common engineering assumptions arise, uncover how problems are linked, and postulate open challenges.

Copyright © 2022 The Authors. This is an open access article under the CC BY-NC-ND license (https://creativecommons.org/licenses/by-nc-nd/4.0/)

Keywords: Energy management, inverters, (non)linear optimization, optimal control.

1. INTRODUCTION

Power networks all over the world are experiencing dramatic upheaval in compositional form and anticipated functionality. With retirement of fossil-fuel-driven synchronous generators, integration of renewable energy, and adoption of electrified transportation, there is a pronounced change in the types and numbers of energy-conversion interfaces that form the backbone of the grid [Taylor et al. (2016)], [Kroposki et al. (2017)]. Particularly, energy processing in future grids will be dominantly handled by semiconductor-based power-electronics circuits termed inverter-based resources (IBRs).

In power networks, the nodal power/current injections, voltages, and edge power/current flows abide by Ohm's and Kirchoff's laws. Generally stated, energy-management tasks aspire to optimally control a subset of these network quantities such that the remaining resultant quantities are within desired limits; optimality is quantified based on cost of resources, or network attributes such as losses and voltage deviations. Managing energy in electric networks with IBRs is a challenging undertaking [Milano et al. (2018)]. This has to be accomplished while acknowledging dynamics cutting across multiple timescales, in the face of uncertainty, and potentially with competing interests from operators and owners. Literature in energy management for synchronous-generator-based resources is a mature

topic; that devoted to IBRs is growing, albeit scattered. Particularly lacking are rigorous attempts to tie together problem formulations across timescales and complexity. These are the precise gaps that our work addresses.

We present a suite of energy-management problems tailored to IBRs of two types: grid-following (GFL) and grid-forming (GFM). GFL IBRs are the de facto technology today; they involve phase-locked loops to synchronize with grids and follow the sensed terminal voltage. On the other hand. GFM resources can form voltages in the absence of other resources; they can offer improved stability margins, and therefore, are anticipated to dominate in number and capacity in future grids [Milano et al. (2018); Venkatramanan et al. (2022)]. Our examination of energy-management problems in networks involving both technologies is motivated by the projection of their coexistence in the near term. We classify problems based on timescales and complexity into four broad categories ranging from infinite-dimensional optimal-control problems to stochastic linear programs (see Fig. 1). For each, we outline companion models for the network and resources. Traversal across formulations is undertaken from methodological and analytical view points with controland circuit-theoretic frameworks. Central to our effort is a controlled voltage-source model for GFM & GFL IBRs: appropriate instances of which feature across all problem formulations.

The paper begins with a high-level network model in Section 2; this facilitates the presentation of the suite of problems in Section 3. Detailed companion dynamic and steady-state models for IBRs compatible with the problem settings and corresponding linearizations are given in Section 4. (Material in Sections 2–3 is presented in a self-contained manner to preserve generality.) A discussion of open challenges in Section 5 rounds off the paper.

^{*} This work was authored in part by NREL, operated by Alliance for Sustainable Energy, LLC, for the US Department of Energy (DOE) under Contract No. DE-AC36-08GO28308. Funding provided by DOE Office of Energy Efficiency and Renewable Energy under Solar Energy Technologies Office (SETO) through the UNIFI Consortium and Agreement EE0009025; from the National Science Foundation grants 1444745, 1901134, 2126052; and UMN's MnDRIVE program is also gratefully acknowledged.

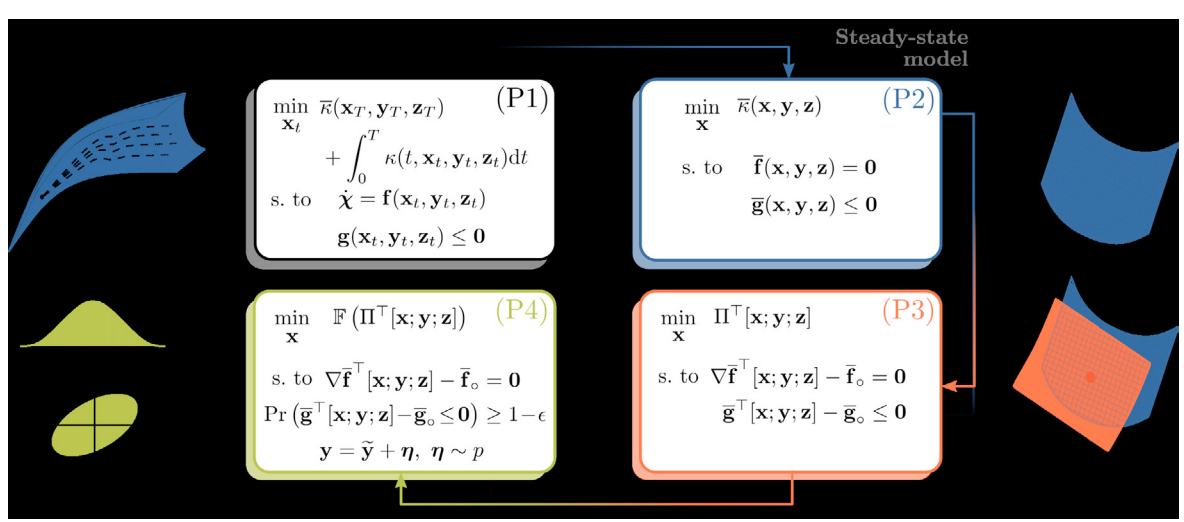


Fig. 1. Illustrating the suite of energy-management problems discussed in Section 3. Assumptions and simplifications that facilitate traversing across the problems are also listed alongside. Problem (P1) pertains to dynamic operating conditions, while (P2)–(P4) apply to steady-state operation.

2. POWER NETWORK MODEL

To capture the dynamic and steady-state characteristics of a network hosting IBRs, this section develops appropriate models. We consider a three-phase balanced RL network with N nodes and E edges. The network is modeled as a directed graph $\mathcal{G} = (\mathcal{N}, \mathcal{E})$ with node set $\mathcal{N} = \{1, \ldots, N\}$ and edge set \mathcal{E} . Arbitrarily assigning the directions for edges $e \in \mathcal{E}$, the topology of \mathcal{G} is captured by the incidence matrix $\mathbf{B} \in \{0, \pm 1\}^{N \times E}$ with entries $B_{k,e} = 1(-1)$ if k = m(n) when $\exists e = (m, n) \in \mathcal{E}$; and $B_{k,e} = 0$, otherwise. The IBRs are assumed to be voltage-source inverters with output RL filters. (Details can be found in [Yazdani and Iravani (2010)]; they are not essential to appreciate the system-theoretic constructs introduced in the remainder.)

Construct $E \times E$ diagonal matrices $(\mathbf{R}^{\mathcal{N}}, \mathbf{L}^{\mathcal{N}})$ with the diagonal entries representing the line resistances and inductances, respectively. Similarly, the $N \times N$ diagonal matrices $(\mathbf{R}^{\mathcal{I}}, \mathbf{L}^{\mathcal{I}})$ collect the resistances and inductances of the inverter-network interconnections. Three-phase signals are projected on to a reference frame rotating at electrical-radian synchronous frequency, ω_s (2 π 60 or 2 π 50 Hz) via the Park's transformation [Yazdani and Iravani (2010)]. Collect the ensuing complex-valued node voltages, current injections, and inverter terminal voltages in N-length vectors, $\mathbf{V}, \mathbf{I}, \mathbf{E}$; and line currents in the E-length vector, \mathbf{F} . The RL dynamics for the network dictates

$$\mathbf{L}^{\mathcal{N}} \frac{\mathrm{d}\mathbf{F}}{\mathrm{d}t} = \mathbf{B}^{\mathsf{T}} \mathbf{V} - \mathbf{R}^{\mathcal{N}} \mathbf{F} - \jmath \omega_{\mathrm{s}} \mathbf{L}^{\mathcal{N}} \mathbf{F}. \tag{1}$$

Current injections and flows are related via Kirchoff's current law (KCL), compactly captured by

$$I = BF. (2)$$

The RL dynamics of the inverter output-filter interconnections can be expressed as:

$$\mathbf{L}^{\mathcal{I}} \frac{\mathrm{d}\mathbf{I}}{\mathrm{d}t} = \mathbf{E} - \mathbf{V} - \mathbf{R}^{\mathcal{I}} \mathbf{I} - \jmath \omega_{\mathrm{s}} \mathbf{L}^{\mathcal{I}} \mathbf{I}. \tag{3}$$

The active and reactive power injected by the inverters at their terminals are captured in real-valued vectors (\mathbf{P}, \mathbf{Q}) , and we express $\mathbf{S} = \mathbf{P} + \jmath \mathbf{Q}$. It follows:

$$\mathbf{S} = \frac{3}{2}\mathbf{E} \circ \mathbf{I}^*,\tag{4}$$

where \circ represents element-wise vector products, and $(\cdot)^*$ denotes the complex conjugate. Focusing on the IBR dynamics, \mathbf{E} is a controlled voltage source representing the terminal behavior of the IBR. It derives from complex-valued vector \mathbf{E}' , entries of which are synthesized by individual inverters and transformed to sinusoids rotating at frequencies $\boldsymbol{\omega}$:

$$\boldsymbol{\omega} = \mathbf{1}\omega_{\mathrm{s}} + \frac{\mathrm{d}\boldsymbol{\varphi}'}{\mathrm{d}t},\tag{5}$$

where φ' is a controller state variable with initial condition $\varphi'_0 = \varphi'(t=0)$. Vectors **E** and **E'** are related via ¹

$$\mathbf{E} = \mathbf{E}' \circ e^{j(\boldsymbol{\varphi}' - \boldsymbol{\varphi}'_0)}. \tag{6}$$

The control laws that dictate the synthesis of \mathbf{E}' and the dynamics of φ' depend on IBR type (i.e., GFM or GFL), and are detailed in Section 4.1. In particular, we will see that dynamics for inverter at node $n \in \mathcal{N}$ can be expressed in the general form

$$\frac{\mathrm{d}\boldsymbol{\chi}_n}{\mathrm{d}t} = \mathbf{f}_n(\boldsymbol{\chi}_n, P_n^{\star}, Q_n^{\star}, V_n', I_n'), \tag{7a}$$

$$\mathbf{0} = \mathbf{g}_n(\boldsymbol{\chi}_n, P_n^{\star}, Q_n^{\star}, I_n'), \tag{7b}$$

where vector χ_n collects internal states for inverter dynamics (including E'_n, φ'_n as entries); I'_n is the inverter current; power setpoints are denoted as $(P_n^{\star}, Q_n^{\star})$. Equations (1)–(7) adequately model the dynamics of an RL network hosting inverters. Figure 2(a) illustrates the constructs introduced thusfar. Next, we will obtain a corresponding steady-state model.

Steady-state model: In (1)–(7), all grid variables are timevarying signals. We next delve into the scenario, wherein, given some initial operating conditions and references ($\mathbf{P}^{\star}, \mathbf{Q}^{\star}$), the inverter and network dynamics evolve to a steady state. Pertinent fundamental questions include: q1)

 $^{^1}$ Frequently in the literature, complex-valued quantities obtained from applying Park's transformation at $\omega_{\rm s}$ are referred as global DQ variables, while those obtained via Park's transformation at local frequencies in ω are referred as local dq variables. Typically, the global DQ frame is used to express network-related quantities, while local dq frames are used for resource-specific quantities. All quantities marked $(\cdot)'$ in the remainder are expressed in local dq frames, and thus are associated with transformations resembling (6).

Whether a stable steady-state operating point exists; and q2) Given an initial operating condition, will the system dynamics attain steady-state operation. While addressing q1)-q2) is beyond the scope of this work, existing literature provides relevant findings and open problems based on analytical and empirical studies [Barklund et al. (2008)], [Dörfler et al. (2016)], [Xin et al. (2011)]. Assuming affirmative answers to q1)-q2), steady-state operation dictates that signals V, E, I, and F correspond to constant-magnitude phasors at a common steady-state frequency, ω_{ss} . Analysis of such operation is facilitated by defining static complex vectors $(\overline{\mathbf{V}}, \overline{\mathbf{E}}, \overline{\mathbf{I}}, \overline{\mathbf{F}})$ by multiplying $(\mathbf{V}, \mathbf{E}, \mathbf{I}, \mathbf{F})$ with $e^{j(\omega_{ss} - \omega_{s})t}$. The aforementioned definitions allow writing (1)–(3) as algebraic relations:

$$\overline{\mathbf{E}} - \overline{\mathbf{V}} = (\mathbf{R}^{\mathcal{I}} + \jmath \omega_{ss} \mathbf{L}^{\mathcal{I}}) \overline{\mathbf{I}}, \tag{8a}$$

$$\overline{\mathbf{I}} = \mathbf{B}\overline{\mathbf{F}},$$
 (8b)

$$\mathbf{I} = \mathbf{BF}, \tag{8b}$$

$$\mathbf{B}^{\top} \overline{\mathbf{V}} = (\mathbf{R}^{\mathcal{N}} + \jmath \omega_{\rm ss} \mathbf{L}^{\mathcal{N}}) \overline{\mathbf{F}}. \tag{8c}$$

To obtain a steady-state model for inverters, one could set $\dot{\chi}_n = \mathbf{0}$ in (7). However, in steady state, network operators may not be concerned with the internal states χ_n 's and signals $(\mathbf{E}', \mathbf{I}')$. Thus, a simpler model may be obtained to replace (5)–(7) with the form

$$\overline{\mathbf{f}}_n(\overline{E}_n, \overline{I}_n, P_n^{\star}, Q_n^{\star}, \omega_{ss}) = \mathbf{0}, \tag{9}$$

where the function $\overline{\mathbf{f}}_n$ is parametrized by a set of known parameters of the inverter at node n; see Section 4.2. Figure 2(b) illustrates the steady-state model.

Collectively, (4), (8)-(9) are nonlinear. To formulate computationally tractable energy-management problems, a linear counterpart is desirable. We develop the sought linear model in Section 4.3. It eliminates variables $(\overline{\mathbf{V}}, \overline{\mathbf{I}})$, substituting (4), (8)-(9) by a compact form ²

$$\mathbf{H}\left[\overline{\mathbf{E}}; \mathbf{P}^{\star}; \mathbf{Q}^{\star}; \omega_{ss}\right] + \mathbf{h} = \mathbf{0},\tag{10}$$

where matrix \mathbf{H} and vector \mathbf{h} depend on network and inverter parameters. An affine relation between actual steady-state power injections $\overline{\mathbf{S}}$ and references $\mathbf{S}^{\star} = \mathbf{P}^{\star} +$ ${}_{1}\mathbf{Q}^{\star}$ will also be derived from (9), that takes the form

$$\widetilde{\mathbf{H}}\left[\overline{\mathbf{S}}; \mathbf{S}^{\star}; \overline{\mathbf{E}}; \omega_{\mathrm{ss}}\right] + \widetilde{\mathbf{h}} = \mathbf{0},$$
 (11)

where $(\widetilde{\mathbf{H}}, \widetilde{\mathbf{h}})$ depend on inverter parameters.

3. SUITE OF ENERGY-MANAGEMENT PROBLEMS

In this section, we outline a suite of energy-management problems, abstractions of which are illustrated in Fig. 1. For the exposition to follow, we consider that the setpoints $(P_n^{\star}, Q_n^{\star})$ for IBRs at nodes $n \in \mathcal{N}_L \subset \mathcal{N}$ are given; and the setpoints for the remaining nodes $n \in \mathcal{N}_G =$ $\mathcal{N} \setminus \mathcal{N}_L$ are controllable. Thus, set \mathcal{N}_L represents inelastic/uncontrollable resources, while the nodes in \mathcal{N}_G host the resources to be dispatched while ensuring acceptable network operation. By acceptable operation, we seek that voltages V and frequencies ω are within stipulated limits.

3.1 Finite-horizon Optimal-control Problem

Under the described setup, one could ideally aspire to optimize over trajectories of reference setpoints for a finite time horizon $t \in [0,T]$ while constrained by model dynamics. The ensuing optimal control problem can be posed in the so-called *Bolza* form:

$$\min \sum_{n \in \mathcal{N}_{G}} \overline{c}_{n}(P_{n}(T), Q_{n}(T))$$

$$+ \int_{t=0}^{T} c_{n}(P_{n}(t), Q_{n}(t)) dt \qquad (P1)$$
over $\{P_{n}^{\star}(t), Q_{n}^{\star}(t)\}_{n \in \mathcal{N}_{G}}, \qquad t \in [0, T]$
given $\{P_{n}^{\star}(t), Q_{n}^{\star}(t)\}_{n \in \mathcal{N}_{L}}, \qquad t \in [0, T]$
s.to $(1) - (7)$, and
$$\omega_{\min} \mathbf{1} \leq \omega(t) \leq \omega_{\max} \mathbf{1}, \qquad t \in [0, T] \quad (12a)$$

$$\mathbf{V}_{\min} \leq |\mathbf{V}(t)| \leq \mathbf{V}_{\max}, \qquad t \in [0, T] \quad (12b)$$

where, the first and second terms in the objective function represent the terminal and running payoffs, respectively. Setting $\bar{c}_n(\cdot) = 0$ yields the Lagrange form, while $c_n(\cdot) = 0$ brings (P1) to Mayer form. The formulation (P1) (particularly, the Lagrange form) is pertinent to high-volatility settings where the node power references are functions of time, and the network is modeled via the DAE (1)-(7). For such settings, the frequency and voltage limits are enforced at all times; see (12a)-(12b). Problem (P1) optimizing over functionals $(P_n^{\star}(t), Q_n^{\star}(t))$ for $n \in \mathcal{N}_G$ is infinite dimensional, and hence challenging to solve. To obtain a finite-dimension approximation to (P1), two popular approaches include time discretization [Gan et al. (2000)], and limiting the feasible function space to one spanned by a finite polynomial basis [Khatami et al. (2020)].

In some settings, a network operator may seek to dispatch inverters in \mathcal{N}_G with references $(P_n^{\star}, Q_n^{\star})$ that are constant for $t \in [0, T]$, given time-invariant $(P_n^{\star}, Q_n^{\star})$ for $n \in \mathcal{N}_L$. Once an optimal setpoint is determined, dispatched, and set, the network would evolve per the dynamic models. In such cases, the dimensionality of (P1) reduces while retaining the dynamics in constraints, yielding a finitedimensional optimal-control problem.

3.2 Non-convex Optimization with Steady-state Models We now separate the time scales of network-IBR dynamics

and the intervals at which IBRs are dispatched. A common assumption in so doing is that once optimal setpoints are implemented, say at time t=0, the network-IBR system attains a steady state at a time $t = t_{ss}$. The system stays at this steady-state operating point, before being re-dispatched at time t = T. If $t_{\rm ss} \ll T$, one may simplify (P1) to an algebraic optimization problem by replacing the DAE-constraint set (1)-(7) with the steadystate counterpart (4), (8)-(9); and enforcing the voltagemagnitude and frequency limits (12a)-(12b) under steadystate conditions. The ensuing formulation follows:

$$\min \sum_{n \in \mathcal{N}_{G}} c_{n}(\overline{P}_{n}, \overline{Q}_{n}) \tag{P2}$$

$$\text{over } \{P_{n}^{\star}, Q_{n}^{\star}\}_{n \in \mathcal{N}_{G}},$$

$$\text{given } \{P_{n}^{\star}, Q_{n}^{\star}\}_{n \in \mathcal{N}_{L}},$$

$$\text{s.to } (4), (8) - (9), \text{ and}$$

$$\omega_{\min} \leq \omega_{\text{ss}} \leq \omega_{\max},$$

$$\mathbf{V}_{\min} \leq |\overline{\mathbf{V}}| \leq \mathbf{V}_{\max}. \tag{13a}$$

Familiar instances of (P2) include economic dispatch, or more generally, AC Optimal Power Flow (AC-OPF). Thus, (P2) generalizes the classical AC-OPF formulations to include inverter models. Furthermore, it innovatively models

 $[\]overline{{}^2 \text{ For}}$ vectors \mathbf{x} and \mathbf{y} , $[\mathbf{x}; \mathbf{y}]$ denotes the concatenation $[\mathbf{x}^\top \ \mathbf{y}^\top]^\top$.

the grid to exhibit an unknown steady-state frequency rather than invoking the popular fixed nominal frequency assumption. It is worth pointing that the past decades witnessed tremendous advancements towards obtaining convex relaxations and distributed algorithms for AC-OPF formulations that emerge as simplifications of (P2) (with fixed frequency); see, e.g., [Molzahn et al. (2017)].

3.3 Linearized Optimization with Steady-state Models

The nonlinear equality constraints (4), (8)-(9) render (P2) nonconvex. Linear approximations to the classical AC-OPF problems, viz. DC-OPF in transmission systems and LinDistFlow model of [Baran and Wu (1989)] in distribution systems, are frequently leveraged for computational ease. Along similar lines, one may set up the following linear approximation of (P2):

$$\min \sum_{n \in \mathcal{N}_{G}} c_{n}^{P} \overline{P}_{n} + c_{n}^{Q} \overline{Q}_{n}$$

$$\text{over } \{P_{n}^{\star}, Q_{n}^{\star}\}_{n \in \mathcal{N}_{G}},$$

$$\text{given } \{P_{n}^{\star}, Q_{n}^{\star}\}_{n \in \mathcal{N}_{L}},$$

$$\text{s.to } (10) - (11), \text{ and}$$

$$\omega_{\min} < \omega_{\text{ss}} < \omega_{\max},$$

$$(14a)$$

$$\mathbf{E}_{\min} \le |\overline{\mathbf{E}}| \le \mathbf{E}_{\max},$$
 (14b)

where (c_n^P, c_n^Q) are the linear (re)active power cost coefficients for injection at node n. The linearization adopted in (P3), and detailed in Section 4.3, eliminates the variables $(\overline{\mathbf{V}}, \overline{\mathbf{I}})$; and thus the voltage-magnitude limits (14b) are enforced on the inverter terminal voltages $\overline{\mathbf{E}}$. If needed, one can obtain linearizations to include $(\overline{\mathbf{V}}, \overline{\mathbf{I}})$ in modeling, and subsequently enforce limits on those. Optimal inverter dispatch formulations widely reported in the literature incorporate the LinDistFlow with limited regard offered to modeling resource behavior and frequency variability. The linearization in (P3) overcomes such modeling deficits, while preserving the linear program (LP) problem class.

Problem (P3), being an LP, serves as a gateway to several practical and tractable stochastic energy-management problems. Specifically, network operators may have access to uncertain predictions $(\widetilde{P}_n^{\star},\widetilde{Q}_n^{\star})$ for uncontrollable nodes $n \in \mathcal{N}_L$. A generic stochastic-optimization problem dispatching the inverters $n \in \mathcal{N}_G$ takes the form:

$$\min \sum_{n \in \mathcal{N}_G} \mathbb{F}(c_n^P \overline{P}_n + c_n^Q \overline{Q}_n) \qquad (P4)$$
over $\{P_n^{\star}, Q_n^{\star}\}_{n \in \mathcal{N}_G}$,
given $\{\widetilde{P}_n^{\star}, \widetilde{Q}_n^{\star}\}_{n \in \mathcal{N}_L}$,
s.to $(10) - (11)$, and
$$\Pr(\omega_{\min} \leq \omega_{ss} \leq \omega_{\max}) \geq 1 - \epsilon_{\omega}, \qquad (15a)$$

$$\Pr(\mathbf{E}_{\min} \le \omega_{ss} \le \omega_{\max}) \ge 1 - \epsilon_{\omega}, \tag{15a}$$

$$\Pr(\mathbf{E}_{\min} \le |\overline{\mathbf{E}}| \le \mathbf{E}_{\max}) \ge 1 - \epsilon_{E}, \tag{15b}$$

$$[P_n^* \ Q_n^*] = [\widetilde{P}_n^* \ \widetilde{Q}_n^*] + [\eta_n^P \ \eta_n^Q], \quad \forall n \in \mathcal{N}_L \quad (15c)$$

$$[P_n^{\star} \ Q_n^{\star}] = [P_n^{\star} \ Q_n^{\star}] + [\eta_n^P \ \eta_n^Q], \quad \forall n \in \mathcal{N}_L \quad (15c)$$

 $\{(\eta_n^P, \eta_n^Q)\}_{n \in \mathcal{N}_L} \sim p,$ (15d)

where, the deviations (η_n^P, η_n^Q) in the power references at uncontrolled nodes follow a probability distribution p. If the distribution p has unbounded support (e.g., Gaussian uncertainty), one cannot enforce deterministic voltage-magnitude and frequency limits, thus necessitating chance constraints as in (15a)-(15b). See [Jabr (2019)], [Dall'Anese et al. (2015)], [Kekatos et al. (2015)]. Two

prominent off-shoots of (P4) include:

1) Robust optimization. Assuming p has a bounded support with uniform probability (e.g., polytopic uncertainty), constraint (15d) simplifies to $\{(\eta_n^P, \eta_n^Q)\}_{n \in \mathcal{N}_L} \in \mathcal{U}$, where \mathcal{U} is the support of p. Constraints (15a)-(15b) can be made deterministic by setting $\epsilon_{\omega} = \epsilon_{E} = 0$. Finally, the objective function can be defined as the worst-case cost

$$\mathbb{F}(c_n^P \overline{P}_n + c_n^Q \overline{Q}_n) := \max_{\{\eta_n^P, \eta_n^Q\}} (c_n^P \overline{P}_n + c_n^Q \overline{Q}_n).$$

2) Chance-constrained optimization. For distribution p with unbounded support, one can pick $0 < \epsilon_{\omega}, \epsilon_{E} < 1$ based on the constraint-violation risk appetite. Under such settings, a prevalent choice for the objective function is the expected cost $\mathbb{F}(\cdot) := \mathbb{E}_p(\cdot)$. For tractability, one may need to resort to suitable restrictions/relaxations that enforce the probability of satisfaction in (15a)-(15b) per constraint, instead of constraint groups.

4. MODEL SPECIFICS

The dynamic and steady-state IBR-network models developed in Section 2 are schematically represented in Fig. 2. These high-level models conveniently represent IBRs as controlled voltage sources [Venkatramanan et al. (2022)]. This section provides detailed GFM and GFL models adhering to form (7) under dynamic conditions; and to form (9) in steady state. (These models are ubiquitously referenced in the IBR literature. That said, the previous sections can be read independently of the content furnished here.) Linearizations of form (10) are also made explicit.

4.1 Dynamic Models

Grid-forming Inverter The model discussed below admits (under certain parametric assumptions) three popular GFM-IBR control dynamics: droop, virtual synchronous machine, and dispatchable virtual oscillator control [Ajala et al. (2021); Johnson et al. (2022)]. The model includes dynamics of voltage E'_n , frequency ω_n , and a power filter:

$$\tau_{\mathbf{e}} \frac{\mathrm{d}E_n'}{\mathrm{d}t} = \left(f_{\mathbf{e}}(E_n', |E_n^{\star}|) - \kappa_{\mathbf{e}} \Im(S_n^f - S_n^{\star}) \right), \tag{16}$$

$$\frac{\mathrm{d}\varphi_n'}{\mathrm{d}t} = -\tau_{\mathrm{f}}\omega_n \frac{\mathrm{d}\omega_n}{\mathrm{d}t} + \kappa_{\mathrm{f}}\Re(S_n^f - S_n^*),\tag{17}$$

$$\tau_{\rm p} \frac{\mathrm{d}S_n^f}{\mathrm{d}t} = S_n' - S_n^f,\tag{18}$$

where, $\tau_{\rm e}$, $\tau_{\rm f}$, and $\tau_{\rm p}$ denote the time constants for the voltage, frequency, and power-control loops, respectively. Variable $|E_n^{\star}|$ denotes the voltage-magnitude setpoint, and S_n^f denotes low-pass-filtered measurements of active and reactive powers, κ_e and κ_f capture the voltage- and frequency-droop coefficients of the primary controller; and function $f_{\rm e}(\cdot,\cdot)$ is a difference metric.³

Grid-following inverter The GFL inverter employs a synchronous-reference-frame phase-locked loop (PLL) for grid synchronization and a PI current controller for reference tracking [Yazdani and Iravani (2010)]. The inverter terminal voltage, E'_n , and dynamics of φ'_n are given by:

$$E'_{n} = \left(K_{I}^{p} \frac{\mathrm{d}\Gamma'_{I}}{\mathrm{d}t} + K_{I}^{i} \Gamma'_{I}\right),\tag{19}$$

³ Apparent power is invariant to reference-frame transformations, i.e., $\mathbf{S}' = \mathbf{S}$. This can readily be verified: $\mathbf{S}' = \frac{3}{2}\mathbf{E}' \circ (\mathbf{I}')^* =$ $\frac{3}{2}e^{-\jmath(\boldsymbol{\varphi}'-\boldsymbol{\varphi}'_0)}\circ\mathbf{E}\circ\left[e^{-\jmath(\boldsymbol{\varphi}'-\boldsymbol{\varphi}'_0)}\circ\mathbf{I}\right]^*=\mathbf{S}.$

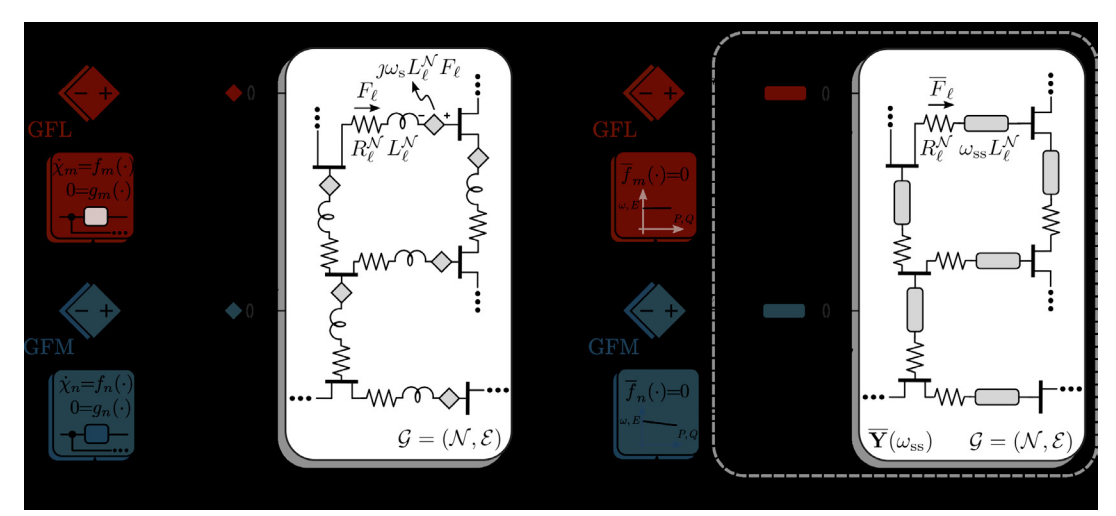


Fig. 2. (a) Dynamic & (b) steady-state network circuit model with IBRs represented as controlled voltage sources.

$$\frac{\mathrm{d}\varphi_n'}{\mathrm{d}t} = K_{PLL}^{\mathrm{p}} \frac{\mathrm{d}\phi_n'}{\mathrm{d}t} + K_{PLL}^{\mathrm{i}} \phi_n'. \tag{20}$$

The PI control loops in (19) and (20) are closed around the measured inverter current, I'_n , and grid voltage, V'_n :

$$\frac{\mathrm{d}\phi_n'}{\mathrm{d}t} = -\Re(V_n'),\tag{21}$$

$$\frac{\mathrm{d}\Gamma_I'}{\mathrm{d}t} = I_n'^* - I_n' = \left(\frac{S_n^*}{E_n'}\right)^* - I_n',\tag{22}$$

where, current reference, $I_n^{\prime\star}$, is derived from S_n^{\star} .

Remark 1. Mapping the inverter dynamic models to (7), the dynamic state variables χ_n for GFM and GFL are $[E'_n; \varphi'_n; \omega_n; S^f_n]$ and $[\Gamma'_I; \varphi'_n; \phi'_n]$, respectively. The DAE (7) for GFM comprises of (16)-(18) and (4); and for GFL it is formed by (19)-(22). In (16)-(22), some inverter parameters have not been indexed by n to keep the notation uncluttered. These, however may vary per inverter.

4.2 Steady-state Models

Grid-forming Inverter The algebraic relationships capturing the steady-state operation of a GFM at node n are:

$$\overline{Q}_n \approx Q_n^{\star} - M_Q^{-1}(|\overline{E}_n| - |E_n^{\star}|), \tag{23}$$

$$\overline{P}_n = P_n^{\star} - M_P^{-1}(\omega_{\rm ss} - \omega_{\rm s}), \tag{24}$$

where, (M_Q, M_P) are droop coefficients inferred from the dynamic model. We obtain (23) by linearizing (16) in steady-state, where, $\overline{Q}'_n = Q'_n = Q_n$, and recognizing that $|\overline{E}_n| = |E'_n|$. Similarly (24) is obtained from (17) with $\overline{P}'_n = P'_n = P_n$ and setting $\dot{\varphi}'_n = \omega_{\rm ss} - \omega_{\rm s}$ (see (5)).

Grid-following inverter Algebraic expressions pertinent to steady-state operation follow from (22) as:

$$[\overline{P}_n \ \overline{Q}_n] = [P_n^{\star} \ Q_n^{\star}]. \tag{25}$$

The steady-state models (23)-(24), and (25), alongside (4), comply with the general form (9). Moreover, (23)-(25) relate the reference and steady-state injected powers as per the desired linear form of (11).

4.3 Linearized Steady-state Network Model

In steady state, one can substitute $\overline{\mathbf{V}}$ from (8a) in (8c) and solve for $\overline{\mathbf{F}}$. Subsequently, using (8b) provides

$$\overline{\mathbf{I}} = \underbrace{\mathbf{B}(\mathbf{R}^{\mathcal{N}} + \jmath \omega_{\mathrm{ss}} \mathbf{L}^{\mathcal{N}})^{-1} \mathbf{B}^{\top}}_{\overline{\mathbf{Y}}(\omega_{\mathrm{ss}})} [\overline{\mathbf{E}} - (\mathbf{R}^{\mathcal{I}} + \jmath \omega_{\mathrm{ss}} \mathbf{L}^{\mathcal{I}}) \overline{\mathbf{I}}],$$

where the matrix $\overline{\mathbf{Y}}(\omega_{ss})$ is the admittance matrix for the network \mathcal{G} . Solving further for current $\overline{\mathbf{I}}$ yields

$$\overline{\mathbf{I}} = \underbrace{\left[\mathbb{I} + \overline{\mathbf{Y}}(\omega_{\rm ss})(\mathbf{R}^{\mathcal{I}} + \jmath \omega_{\rm ss} \mathbf{L}^{\mathcal{I}})\right]^{-1} \overline{\mathbf{Y}}}_{\mathbf{Y}(\omega_{\rm ss})} \overline{\mathbf{E}}, \tag{26}$$

where I is the identity matrix of suitable dimension. Equation (26) relating \overline{I} and \overline{E} is the reduced system description with the equivalent admittance matrix $\mathbf{Y}(\omega_{ss})$.

To obtain a linear model for the IBR-network system, at the outset, one notes that the steady-state behavior of IBRs modeled via (23)–(25) are linear in the variables $(\overline{\mathbf{P}}, \overline{\mathbf{Q}}, \overline{\mathbf{E}}, \omega_{\rm ss})$. The nonlinearity stems from the network governing equation (26) and the definition of injected power (4). Assuming $|\omega_{\rm ss}-\omega_{\rm s}|\ll\omega_{\rm s}$, one can set $\mathbf{Y}(\omega_{\rm ss})\approx\mathbf{Y}(\omega_{\rm s})$, thus eliminating the nonlinearity from (26). Henceforth, matrix $\mathbf{Y}(\omega_{\rm s})$ will simply be denoted as \mathbf{Y} . Finally, we shall linearize the quadratic dependence of apparent power on the voltages $\overline{\mathbf{E}}$ given by $\overline{\mathbf{P}}+\jmath\overline{\mathbf{Q}}\approx\mathrm{diag}(\overline{\mathbf{E}})\mathbf{Y}^*\overline{\mathbf{E}}^*$. To that end, we fix a nominal voltage $e_{\circ}\mathbf{1}$, that allows us to express $\overline{\mathbf{E}}=e_{\circ}\mathbf{1}+\Delta\overline{\mathbf{E}}$, where e_{\circ} is a real scalar, and it is assumed that $|\Delta\overline{E}_n|\ll e_{\circ},\ \forall\ n\in\mathcal{N}$. Following the steps of [Dhople et al. (2015)], yields

$$\begin{bmatrix} \overline{\mathbf{P}} \\ \overline{\mathbf{Q}} \end{bmatrix} = e_{\circ} \begin{bmatrix} \Re(\mathbf{Y}) & -\Im(\mathbf{Y}) \\ -\Im(\mathbf{Y}) & -\Re(\mathbf{Y}) \end{bmatrix} \begin{bmatrix} |\overline{\mathbf{E}}| \\ \angle \overline{\mathbf{E}} \end{bmatrix}.$$
(27)

Equation (27) serves as a linear power-flow model for the network. Substituting $(\overline{\mathbf{P}}, \overline{\mathbf{Q}})$ from (27) in the linear inverter steady-state models (23)-(25) yields (10).

5. OPEN PROBLEMS & CLOSING REMARKS

Described below—in no particular order—are open problems implicit in the formulations (P1)–(P4):

1) Choice of cost functions. Cost functions in classical OPF problems for synchronous generators are typically derived from fuel cost. For IBRs driven by renewables, defining cost functions in this vein is not readily possible since sources such as wind and solar have no fuel costs. Some approaches have suggested tying cost(s) to consumer utility/comfort; yet others have demonstrated how specific choices tied to available capacity can ensure a desired power-provisioning profile. Another option is to recognize capital and O&M costs, and derive cost functions that amortize these across expected life. In general, the limited (to no) participation of IBRs as price makers and lack

- of universally accepted pricing mechanisms for ancillary services in markets have delayed reaching consensus.
- 2) Models & parameterization. Decades of sustained effort from industry and academia has ensured wide acceptance of standardized synchronous-generator models. However, IBR models for different operational tasks are not standardized. This is primarily because IBR-model response characteristics are dictated by (implementation-specific) control algorithms and set points. Since the same level of standardization of these response characteristics has been lacking, models are not as well defined. With growing numbers, models will have to be cast in forms that permit integration in control and optimization frameworks and parameters will have to be sourced from hardware prototypes and translated across power levels.
- 3) Network complexity. Our modeling framework is presented for a balanced three-phase network. In practice, IBRs of varying power ratings are installed and operated by a wide variety of owners and operators (end customers, utilities, developers), and dispersed across transmission and distribution networks. Reduced-order models and aggregations at suitable abstraction levels will be necessary to counter the curses of dimensionality and heterogeneity. 4) Computational complexity. Tremendous efforts have been made towards achieving scalability in solving classical renditions of (P1)-(P4) including distributed and decentralized control and optimization, convex relaxations, and tractable stochastic frameworks. Inclusion of IBR models and allowing frequency variation in (P1)–(P4) challenge the direct applicability of the existing approaches, and call for meticulous retrofitting. Development of novel computational approaches is needed to tractably solve future energy-management problems.
- 5) Secondary control. Grid operations include secondary control mechanisms for restoring frequency to a steady-state synchronous value. The typical approach is to organize cohorts of resources into balancing / control areas and restore frequency and flows across these to nominal and scheduled values, respectively, via distributed integral control. While the motivation of including frequency is well intentioned in (P1)–(P4), there is a need to align energy-management problems with prevailing and up-and-coming architectures for secondary control.
- 6) Stability. The implicit assumption behind time-scale separation imposed between dispatch and real-time control in bulk grids is that underlying dynamics are stable and actuation will not trigger unstable or undesirable behavior. For problems that involve dynamic models (such as (P1)), stability guarantees (or proxies thereof) would appear necessary to guarantee performance. While recognized in passing in the literature, this requires more investigation.

REFERENCES

- Ajala, O., Baeckeland, N., Dhople, S., and Domínguez-García, A. (2021). Uncovering the Kuramoto model from full-order models of grid-forming inverter-based power networks. In *Proc. IEEE Conf. on Decision and Control*, 4944–4949. Austin, USA.
- Baran, M. and Wu, F. (1989). Optimal sizing of capacitors placed on a radial distribution system. *IEEE Trans. Power Syst.*, 4(1), 735–743.
- Barklund, E., Pogaku, N., Prodanovic, M., Hernandez-Aramburo, C., and Green, T.C. (2008). Energy

- management in autonomous microgrid using stability-constrained droop control of inverters. *IEEE Trans. Power Del.*, 23(5), 2346–2352.
- Dall'Anese, E., Dhople, S.V., Johnson, B.B., and Giannakis, G.B. (2015). Optimal dispatch of residential photovoltaic inverters under forecasting uncertainties. IEEE J. Photovoltaics, 5(1), 350–359.
- Dhople, S.V., Guggilam, S.S., and Chen, Y.C. (2015). Linear approximations to AC power flow in rectangular coordinates. In *Proc. Allerton Conf.*, 211–217.
- Dörfler, F., Simpson-Porco, J.W., and Bullo, F. (2016). Breaking the hierarchy: Distributed control and economic optimality in microgrids. *IEEE Trans. Control Netw. Syst.*, 3(3), 241–253.
- Gan, D., Thomas, R., and Zimmerman, R. (2000). Stability-constrained optimal power flow. *IEEE Trans. Power Syst.*, 15(2), 535–540.
- Jabr, R.A. (2019). Robust volt/var control with photo-voltaics. *IEEE Trans. Power Syst.*, 34(3), 2401–2408.
- Johnson, B., Roberts, T.G., Ajala, O., Domínguez-García, A., Dhople, S., Ramasubramanian, D., Tuohy, A., Divan, D., and Kroposki, B. (2022). A generic primary-control model for grid-forming inverters: Towards interoperable operation & control. In *Proc. Hawaii Int. Conf. System Sciences*, 3398–3407.
- Kekatos, V., Wang, G., Conejo, A.J., and Giannakis, G.B. (2015). Stochastic reactive power management in microgrids with renewables. *IEEE Trans. Power Syst.*, 30(6), 3386–3395.
- Khatami, R., Parvania, M., Chen, C., Guggilam, S., and Dhople, S. (2020). Dynamics-aware continuous-time economic dispatch: A solution for optimal frequency regulation. In *Proc. Hawaii Int. Conf. System Sciences*, 3186–3195.
- Kroposki, B., Johnson, B., Zhang, Y., Gevorgian, V., Denholm, P., Hodge, B.M., and Hannegan, B. (2017). Achieving a 100% renewable grid: Operating electric power systems with extremely high levels of variable renewable energy. *IEEE Power and Energy Magazine*, 15(2), 61–73.
- Milano, F., Dörfler, F., Hug, G., Hill, D.J., and Verbič, G. (2018). Foundations and challenges of low-inertia systems. In *Proc. Power Sys. Comp. Conf.*, 1–25.
- Molzahn, D.K., Dörfler, F., Sandberg, H., Low, S.H., Chakrabarti, S., Baldick, R., and Lavaei, J. (2017). A survey of distributed optimization and control algorithms for electric power systems. *IEEE Trans. Smart Grid*, 8(6), 2941–2962.
- Taylor, J.A., Dhople, S.V., and Callaway, D.S. (2016). Power systems without fuel. Renewable and Sustainable Energy Reviews, 57, 1322–1336.
- Venkatramanan, D., Singh, M.K., Ajala, O., Domínguez-García, A., and Dhople, S. (2022). Integrated system models for networks with generators & inverters. arXiv preprint arXiv:2203.08253.
- Xin, H., Qu, Z., Seuss, J., and Maknouninejad, A. (2011). A self-organizing strategy for power flow control of photovoltaic generators in a distribution network. *IEEE Trans. Power Syst.*, 26(3), 1462–1473.
- Yazdani, A. and Iravani, R. (2010). Voltage-Sourced Converters in Power Systems. John Wiley & Sons, Inc., Hoboken, NJ.